

Preparation of the HIV Attachment Inhibitor BMS-663068. Part 3. Mechanistic Studies Enable a Scale-Independent Friedel–Crafts Acylation

Gregory L. Beutner,^{*ID} Jacob Albrecht, Junying Fan, Dayne Fanfair, Michael J. Lawler, Michael Bultman,^{ID} Ke Chen, Sabrina Ivy, Richard L. Schild, Jonathan C. Tripp, Saravanababu Murugesan, Konstantinos Dambalas, Douglas D. McLeod, Jason T. Sweeney, Martin D. Eastgate,^{ID} and David A. Conlon

Chemical & Synthetic Development, Bristol-Myers Squibb Company, One Squibb Drive, New Brunswick, New Jersey, 08903-0191, United States

S Supporting Information

ABSTRACT: During the development of a Friedel–Crafts acylation for the preparation of a key pyrrole intermediate in the synthesis of the HIV attachment inhibitor, BMS-663068-03, a significant scale dependence was found. A precipitous drop in yield was observed for the acylation of a protected pyrrole with chloroacetyl chloride upon scale-up. Spectroscopic studies to mitigate this scale dependence led to the identification of the complex effect of dissolved hydrogen chloride (HCl) as well as the poor reactivity of the acylating agent, chloroacetyl chloride. At this point, the counterintuitive choice to switch to a longer, but scale-independent, three-step route was made. By changing the acylating agent to acetyl chloride, a more robust process was obtained. Rapid development of a high yielding α -chlorination then provided the common α -chloroketone intermediate required to generate the desired α -amide ketopyrrole. The improved yield and scalability of this three-step process supported the addition of one linear step to the route, and it was demonstrated successfully at scale.

INTRODUCTION

The practical synthesis of substituted pyrroles, prominent heterocycles in pharmaceutical products,¹ is limited at large scale due to the lack of availability of simple pyrrole building blocks. Two main strategies are available to prepare these compounds, namely, (a) the de novo synthesis of the pyrrole ring, and (b) the selective functionalization of the parent, unsubstituted pyrrole. Although numerous strategies exist for de novo construction of pyrroles with a variety of substitution patterns,² the functionalization of low-cost, readily available pyrroles remains an attractive alternative. However, due to the fact that pyrroles are ambident nucleophiles,³ their selective functionalization still presents major challenges.⁴ In light of these limitations we set out to prepare 3-substituted pyrrole **5** (Scheme 1). The 3-aminoacetyl group in **5** was a key functional group handle for further elaboration into the pyrrolopyridine core of the target molecule, BMS-663068. Initial plans to synthesize **5** started with readily available *N*-benzenesulfonyl pyrrole **1** (Besyl, Bs = C₆H₅SO₂–). We envisioned that Friedel–Crafts acylation of **1** with chloroacetyl chloride followed by amidation with the sodium salt of *N*-tosylformamide (**4**) would provide efficient access to **5**.⁵ However, in the course of this work, we realized that this two-step protocol presented major concerns for scale-up. Herein, we describe efforts to develop a high-yielding, scale-independent synthesis of **5** as well as lessons learned about balancing empirical and mechanistic methods to accelerate the development process.

RESULTS AND DISCUSSION

Step 1: Friedel–Crafts Acylation of Pyrrole 1. The Friedel–Crafts reaction between **1** and chloroacetyl chloride (ClCH₂COCl) is known to give moderate yields and high C3:C2 selectivity (Scheme 1).⁶ In our hands at 100 g scale, the reaction was homogeneous and took 4–6 h to reach full conversion with no significant exotherm (adiabatic temperature increase <10 °C). Attempts to optimize the process revealed that the order and rate of reagent addition had a significant impact on yield and selectivity. The optimal results were found by first charging AlCl₃ and chloroacetyl chloride to a reactor containing CH₂Cl₂ and then rapidly adding a solution of pyrrole **1** in CH₂Cl₂. The reaction required 5 h to reach full conversion and afforded **2** in 74% yield and 16:1 C3:C2 selectivity (Table 1, entry 1). The remaining 21% of the input pyrrole **1** could not be accounted for. All other permutations of this charge sequence resulted in lower and variable yields. For example, a 5% yield was obtained when a mixture of AlCl₃ and ClCH₂COCl in CH₂Cl₂ was charged to a solution of pyrrole **1** in CH₂Cl₂ (entry 2).

The rate of addition of pyrrole **1** to the mixture of AlCl₃ and ClCH₂COCl was also critical for achieving good yields and selectivity. Thus, charging the solution of **1** over 180 min resulted in a decreased yield and selectivity relative to faster

Special Issue: From Invention to Commercial Process Definition: The Story of the HIV Attachment Inhibitor BMS-663068

Received: March 24, 2017

Published: August 9, 2017

Scheme 1. Synthesis of Pyrrole 5 en Route to BMS-663068

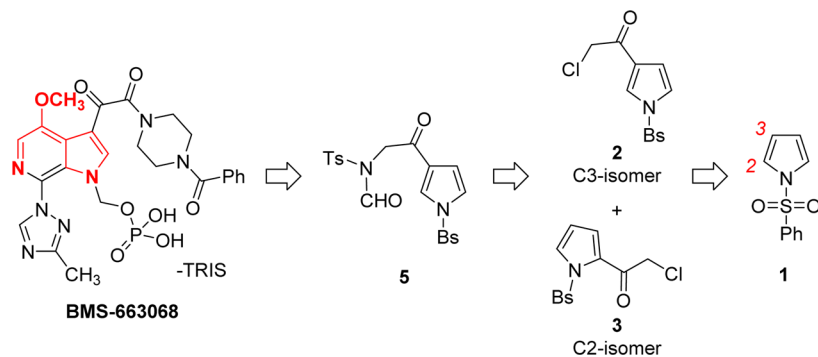


Table 1. Conditions for Friedel–Crafts Acylation of Pyrrole 1

entry	addition order ^a	addition time (min)	yield ^b (%)	2:3 ratio ^b
1	1 to AlCl ₃ /ClCH ₂ COCl	1	74	16:1
2	AlCl ₃ /ClCH ₂ COCl to 1	1	5	ND
3	1 to AlCl ₃ /ClCH ₂ COCl	180	50	2.3:1

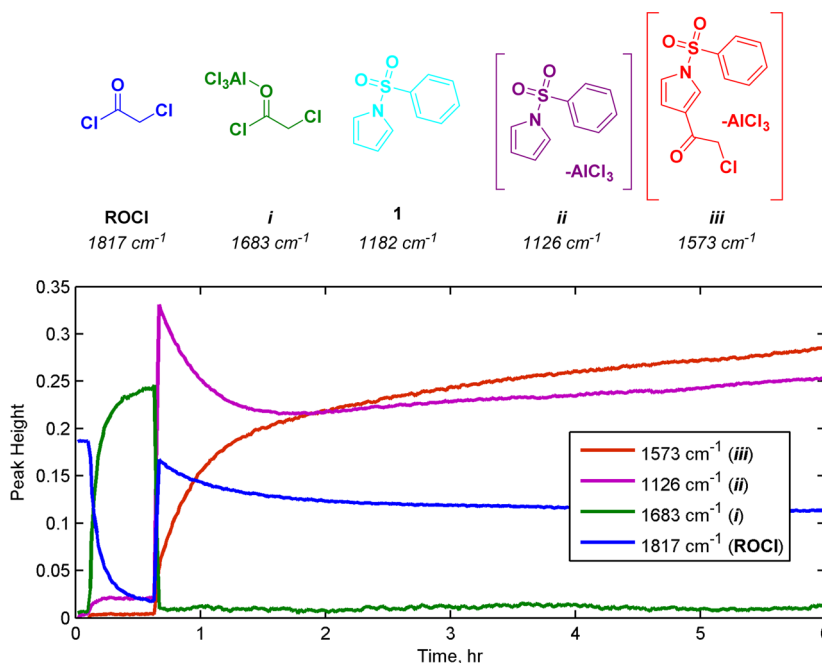
^aReactions run at 16 L/kg DCM relative to 1 with 1.1 equiv of AlCl₃ and 1.2 equiv of ClCH₂COCl at 20 °C. ^bYield and C3:C2 ratio determined by quantitative HPLC measurements.

additions (compare entries 3 and 1). Again, full conversion was observed, but mass recovery was poor. This was common in many reactions of ClCH₂COCl with 1 in our hands.

Although we identified conditions that could provide acceptable yield and selectivity at 100 g scale, the results

were not entirely reproducible, especially as the scale of the reaction increased. Initial attempts at kilogram scale led to yields far below 50% with the remainder of the material being unaccounted for. Since the Friedel–Crafts acylation of 1 with ClCH₂COCl is a relatively slow, homogeneous reaction without a significant exotherm, the usual causes of scale dependent performance, such as mass-transfer limitations or poor heat transfer, did not appear to be at issue here. A Design of Experiments (DoE) study was undertaken to investigate the effect of temperature, reactor headspace, and excess of ClCH₂COCl relative to AlCl₃ on reaction yield and selectivity. The inclusion of temperature and reactor headspace as main factors was deemed important since these are common causes of issues on scale-up.⁷ Analysis of the DoE data revealed that reaction yield was strongly dependent on the charges of ClCH₂COCl and AlCl₃ but insensitive to temperature and headspace.

Guided by the findings of the DoE and the observed importance of the order and rates of reagent charges, the reaction was run under conditions that would maximize yield (1.2 equiv of AlCl₃ and 1.4 equiv of ClCH₂COCl), minimize the volume of the solution charge of pyrrole 1 (2.0 L/kg), add

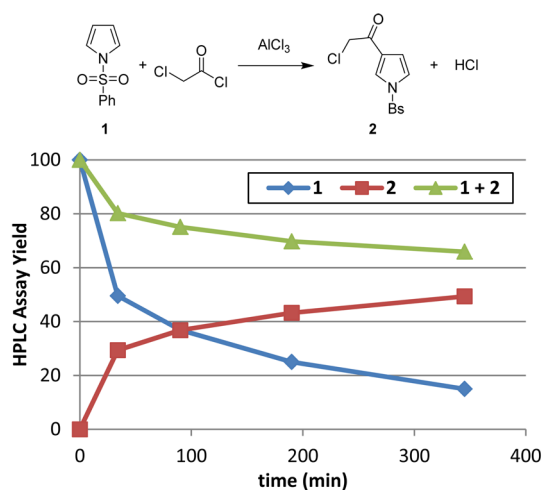
Figure 1. In situ IR monitoring of the reaction of pyrrole 1 and ClCH₂COCl.

the solution of **1** as rapidly as possible subsurface (<15 min), and ensure that the agitation rate was always set to maximum. Despite these changes, the yield decreased from 71% at a 120 kg scale to 35% at a 450 kg scale, even with identical addition times for the solution of pyrrole **1**. These results suggested that there were additional scale-dependent factors that had a significant impact on the performance of this reaction.⁸ At this point, further optimization by DoE could be performed, but unless this unknown factor was included in the design, it seemed unlikely that empirical optimization would provide a path forward to a more robust process. Therefore, we turned to mechanistic studies to better define the reaction pathway and perhaps elucidate the root cause of the scale dependence.

Monitoring the reaction by in situ IR revealed some intriguing trends (Figure 1). Upon mixing ClCH_2COCl with AlCl_3 in 1,2-dichloroethane (DCE),⁹ a slow reaction occurred that led to the dissolution of AlCl_3 . This phenomenon corresponded to the disappearance of the free ClCH_2COCl (1817 cm^{-1}) and the formation of a new signal assigned as the AlCl_3 complex of ClCH_2COCl (i, 1683 cm^{-1}). No signals that could be attributed to an acylium ion at $\sim 2200\text{ cm}^{-1}$ were observed.¹⁰ The addition of **1** to this homogeneous solution led to the instantaneous disappearance of the complex i and regeneration of free ClCH_2COCl . No free pyrrole **1** was observed at 1182 cm^{-1} , but rather a slightly shifted signal appeared at 1126 cm^{-1} . Control experiments performed where **1** was mixed with AlCl_3 showed a similar pattern with a major absorbance at 1126 cm^{-1} , suggesting the formation of an AlCl_3 -complex of the pyrrole ii. The formation of product **2** could be tracked through the growth of a band at 1573 cm^{-1} , which was consistent with the AlCl_3 complex iii. The identity of this signal was confirmed by observation of an analogous spectrum when isolated **2** was mixed with AlCl_3 . It was also observed by IR and HPLC that this complex iii was stable for prolonged periods of time, indicating that the poor mass recovery observed in the reaction was not a consequence of poor product stability under the reaction conditions.

The fact that the addition of pyrrole **1** leads to a rapid and complete consumption of complex i without the formation of product **2** suggests that binding of AlCl_3 to ClCH_2COCl is fairly weak compared to binding with **1**. We wanted to determine if the desired reaction occurs through the AlCl_3 complex of the pyrrole ii or through a typical Friedel–Crafts mechanism via the AlCl_3 -activated complex i. To assess this question, we attempted to prepare complex ii and study its reactivity. However, it was observed that the mixture of **1** and AlCl_3 was unstable and decomposed rapidly to afford pyrrole oligomers and polymers as observed by LC-MS. Based on this finding, we hypothesized that the low mass recovery of the reaction could be due to the rapid formation of the unstable complex ii, which undergoes unproductive polymerization at a rate competitive with the desired Friedel–Crafts acylation over the long reaction times.

Monitoring of the reaction by quantitative HPLC revealed that a significant portion of this unproductive reaction occurred at low conversion (Figure 2). Considering the balanced equation for the Friedel–Crafts reaction, we wondered what role HCl could play in the decomposition process. If HCl present in the reaction affects the stability of **1**, it could help explain the variability at scale. For example, the method of charging moisture-sensitive AlCl_3 could lead to increased HCl levels due to uncontrolled hydrolysis. To test the role of HCl on reaction performance, we conducted an experiment where



Reaction run at 16 L/kg DCM relative to **1** with 1.2 equiv AlCl_3 and 1.4 equiv ClCH_2COCl at 20°C .

Figure 2. Quantitative HPLC monitoring of reaction conversion and mass recovery.

the headspace of the reactor was aggressively swept with dry N_2 to purge HCl. This resulted in complete consumption of pyrrole **1**, but <5% yield of the desired product **2**! Conversely, performing the reaction in a sealed vessel with DCE that had been saturated with anhydrous HCl completely inhibited both the desired reaction and the decomposition of **1**. Mixing AlCl_3 and pyrrole **1** in a saturated solution of anhydrous HCl in DCE¹¹ did not lead to formation of complex ii but gave a different, unidentified species evidenced by a characteristic IR band at 1200 cm^{-1} that was indefinitely stable at RT. The dramatic difference in reaction performance observed between these two extremes attested to the strong effect of HCl.

In fact, these experiments support the hypothesis that HCl may be the scale-dependent factor which was missing from the initial DoE optimization. To further assess the influence of HCl and its interaction with the other variables, a four-factor Definitive Screening Design¹² was conceived to ascertain the relative importance of the reagent charges (AlCl_3 equiv, ClCH_2COCl equiv, CH_2Cl_2 volume, and HCl equiv¹³). An analysis of the results identified HCl as the key factor in controlling yield (Figure 3). An unexpected nonlinear dependence of yield on HCl amount suggested that at low conversion dissolved HCl could be beneficial, whereas at higher

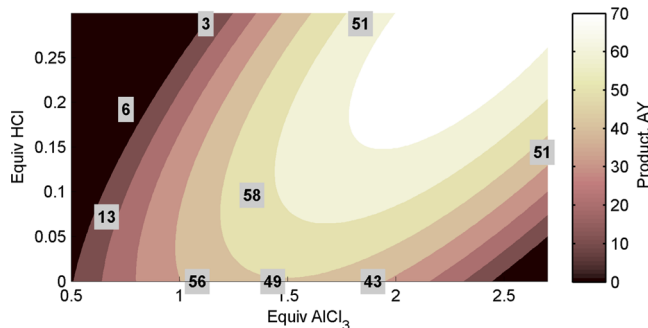


Figure 3. Impact of dissolved HCl and AlCl_3 equivalents on reaction performance. Observed assay yields (%; boxed values) and regressed predictions (contour) revealed a nonlinear relationship between HCl and AlCl_3 .

conversions its presence could be detrimental. Having identified the key factor, we were confident that DoE could provide meaningful answers since we were now posing the correct questions.

On the basis of these results, we propose the reaction mechanism depicted in Figure 4. Although complex **i** is initially

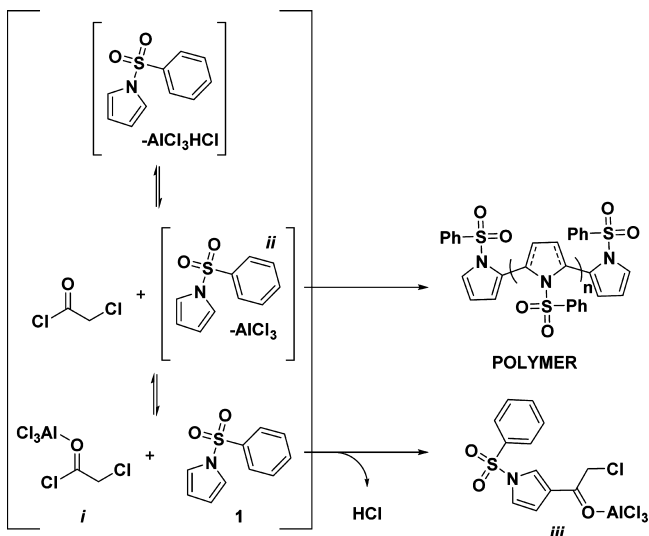


Figure 4. Proposed mechanism for the formation of **2**.

formed upon mixing AlCl_3 and ClCH_2COCl , after addition of pyrrole **1** this complex exists in an equilibrium that strongly favors pyrrole– AlCl_3 complex **ii**. We propose that the desired reaction takes place between complex **i** and **1** via a typical Friedel–Crafts mechanism, rather than the carbometalation route through **ii** as proposed previously.¹⁴ The formation of complex **ii** is unproductive and opens a pathway for polymerization of **1**. The formation of HCl as the reaction proceeds slows the reaction rate but also slows the rate of decomposition of **1**, possibly through stabilization of pyrrole– AlCl_3 complex **ii**. Under low $[\text{HCl}]$, the pyrrole **1** is unstable, while under conditions with higher $[\text{HCl}]$, particularly under conditions where the solution is saturated in HCl , pyrrole **1** is stable, but unreactive. We believe that the dual role of soluble HCl in the reaction is a key factor that influences the scale dependence of the process. Variations in the liquid–gas equilibrium of HCl caused by changes in the volume of the reactor headspace, the rate of exchange of N_2 in the headspace, or the handling of AlCl_3 could affect the amount of HCl and thus the reaction rate and the stability of **1**. Controlling the amount of HCl in the reaction would prove difficult since it is a reaction byproduct, an input related impurity, and strongly affected by the liquid–gas equilibrium in the system.

Having identified the equilibrium between the ClCH_2COCl – AlCl_3 (**i**) and pyrrole– AlCl_3 (**ii**) complexes and the complex role of HCl , we hypothesized that shifting this equilibrium toward the productive complex **i** could improve the reaction yield and rate, and possibly mitigate the scale dependence of the reaction. Toward this end, a wide variety of the reaction conditions were explored including solvents, Lewis acids, and additives. However, these studies revealed that the reaction only tolerates minor changes from the original conditions. Chlorinated solvents were optimal, and only group 13 Lewis acids such as AlCl_3 and GaCl_3 gave reasonable levels of reactivity. The addition of sterically hindered amines, like

2,6-di-*tert*-butylpyridine, led to decreased reactivity as did the addition of various salts such as NaAlCl_4 .

An alternative approach was to consider changing the structure of the electrophile. In general, Friedel–Crafts reactions of sulfonyl pyrroles are reported to be high-yielding transformations,¹⁵ and only in the case of α -chlorinated acid chlorides are lower yields reported.⁶ A wide variety of electrophiles were investigated that would still allow us to access an intermediate which would readily lead to **5** (Figure 5).

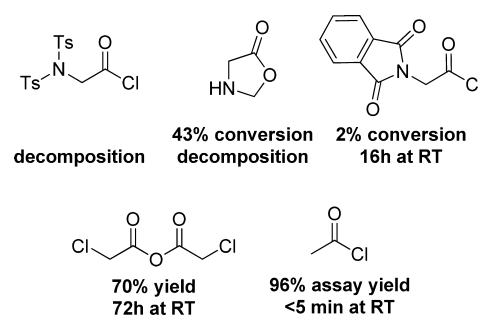


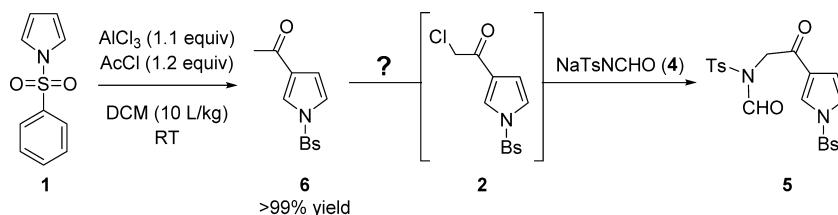
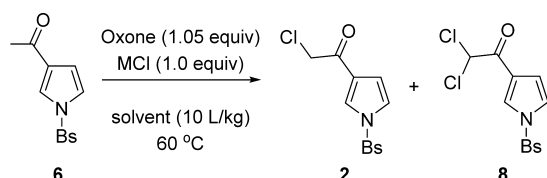
Figure 5. Survey of alternative electrophiles.

The anhydride of chloroacetic acid did not yield any tangible improvements over ClCH_2COCl . Several α -amino acid chlorides were investigated but did not prove successful owing to low conversions. In stark contrast, acetyl chloride (AcCl) showed rapid and quantitative conversion to the desired product.¹⁶ No polymerization of pyrrole **1** could be detected, and in initial scale-up experiments, no loss in performance was observed. The dramatic difference in reactivity between ClCH_2COCl and AcCl is likely a function of the stronger binding of AlCl_3 to AcCl , as can be observed in NMR studies of the binding to AlCl_3 to a variety of acid chlorides.¹⁷ This removes the issues caused by the unproductive AlCl_3 equilibrium between **1** and ClCH_2COCl and allows the Friedel–Crafts acylation to proceed more rapidly than pyrrole polymerization.

With this promising result in hand, the reaction of AcCl with **1** was optimized using a similar DoE to that employed previously during optimization of the ClCH_2COCl reaction. Using a slight excess of AlCl_3 and AcCl relative to **1** allowed for nearly quantitative yields of ketone **6** with greater than 99:1 C3:C2 selectivity and excellent in-process purity (Scheme 2). Furthermore, this reaction was essentially addition-controlled and thus not subject to the scale dependence observed in the original ClCH_2COCl process. However, the integration of this reaction into our synthetic route to **5** would then require a high yielding α -chlorination of ketone **6**, which did not exhibit competitive chlorination of the pyrrole ring.

Step 2. Ketone α -Chlorination. There are numerous literature reports of the α -halogenation of carbonyl compounds.¹⁸ Many reports have utilized copper halides,^{18a} trimethylammonium dichloriodate,^{18b} and 1,3-dichloro-5,5-dimethylhydantoin (DCDMH),^{18c,d} among other methods. Our initial focus was to find a high-yielding and atom economical method for performing the chlorination. For that reason, we were intrigued by two simple reagents reported in the literature: Oxone/ NH_4Cl ¹⁹ and *N*-chlorosuccinimide (NCS).²⁰ The combination of Oxone and NH_4Cl appeared to fit our criteria and gave promising results (Table 2). Optimization studies first focused on the reaction solvent

Scheme 2. Preparation of Pyrrole 5 from Pyrrole 1

Table 2. Conditions for the α -Chlorination of Ketone 6 with Oxone

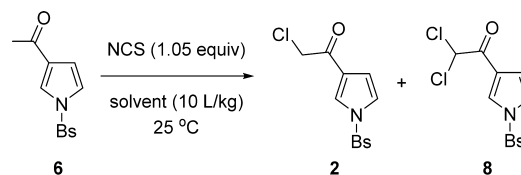
entry	solvent	chloride source	conversion (%)	2:8 (ratio)
1	MeOH	NH ₄ Cl	99	11
2	AcOH	NH ₄ Cl	78	113
3	MeOH/H ₂ O (9:1)	NH ₄ Cl	69	9
4	IPA	NH ₄ Cl	68	6
5	DPMU	NH ₄ Cl	51	5
6	DMF	NH ₄ Cl	49	29
7	CH ₃ CN	NH ₄ Cl	20	179
8	propylene glycol	NH ₄ Cl	20	2
9	sulfolane	NH ₄ Cl	12	35
10	IPAc	NH ₄ Cl	7	25
11	MeTHF	NH ₄ Cl	5	11
12	DCE	NH ₄ Cl	2	17
13	MeOH	Bu ₄ NCl	66	65
14	MeOH	LiCl	73	48
15	MeOH	CsCl	98	18
16	MeOH	CaCl ₂	72	18
17	MeOH	MgCl ₂	52	13
18	MeOH	NaCl	92	10
19	MeOH	KCl	89	8

(entries 1–12). In general, protic and polar solvents gave higher conversions, likely due to the enhanced solubility of Oxone, although no clear trends were apparent. Since MeOH was found to be an optimal solvent for the chlorination, the effect of chloride source was next examined to see if further improvement in terms of selectivity was possible (entries 13–19). In MeOH, the ratio of mono- to dichlorination was significantly higher for Bu₄NCl and LiCl as compared to NH₄Cl, but neither gave high conversion. Therefore, NH₄Cl was selected for further investigation since it gave full conversion and acceptable levels of the dichlorination side product 8.

Further development of the α -chlorination with Oxone and NH₄Cl in MeOH showed that the formation of chloroketone 2 could be achieved in a 55–60% solution yield at 60 °C. The reaction produced the dichloro compound 8 as the major side product along with several other low level impurities. Unfortunately, the reaction stream was not stable, and the level of 8 and other byproducts increased with reaction time and during the subsequent workup. From an engineering perspective, there were several challenges associated with this process. First, Oxone is a relatively dense solid (~1.2 g/mL), and a high loading (3 kg/kg of substrate) was required to

achieve complete conversion of 6. The minimum agitation rate for complete suspension (N_{js}) of Oxone was calculated as 110 rpm \pm 20% for a 3000 L reactor that is half full. This agitation rate is within 8% of the maximum agitation rate for this particular reactor (120 rpm); therefore, it is likely that all of the Oxone will not be completely suspended in the reaction stream. Second, the reaction kinetics were greatly affected by the particle size of Oxone, which means that a size specification would have to be set for this reagent to consistently achieve reaction completion within the desired time. All of these factors were a major challenge for the translation of this chemistry into a robust process.

NCS was explored in the next attempt at devising a robust, high-yielding chlorination. Literature reports describe it as a versatile and convenient reagent, but in our hands it was found to be far less selective than the combination of Oxone and NH₄Cl (Table 3). In CH₂Cl₂, THF, or MeCN, low yields of

Table 3. Conditions for the α -Chlorination of 6 with NCS

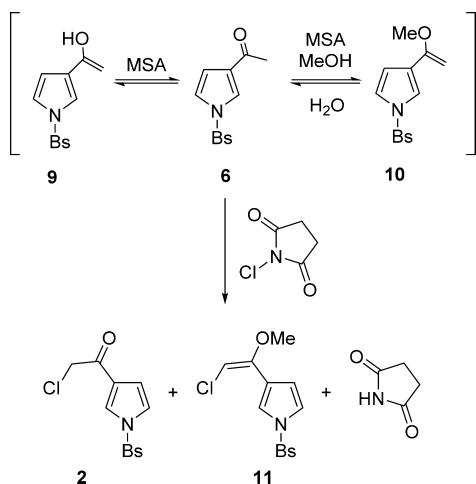
entry	solvent	conversion (%)	yield (2, %)
1	CH ₂ Cl ₂	53	9
2	THF	56	18
3	MeCN	78	10
4	MeOH	>98	93

the desired chloroketone 2 were obtained along with dichlorinated side product 8 and additional ring-chlorinated impurities. However, much to our surprise, the use of MeOH allowed for an efficient chlorination with high selectivity for 2 and an excellent impurity profile. Less than 5% of 8 was formed with no detectable amounts of the ring chlorination byproducts.

Two key factors were found for achieving a high yield in this reaction: NCS equivalents and water content. Elevated levels of 8 were obtained when the NCS charge exceeded 1.1 equiv. Significant amounts of overchlorination products were observed when 1.0 equiv of H₂O was added, which also led to a reduced reaction rate. Thus, it was important to control the NCS charge between 1.05 and 1.10 equiv and water content to below 0.08 equiv. Additional screening revealed that the reaction rate is enhanced by the addition of catalytic amounts of acid. In the presence of 0.1 equiv of methanesulfonic acid (MSA), a significant improvement in rate and yield was observed. Under these optimized conditions, complete conversion was achieved in 6 h at 30 °C with a 90% in-process yield. The safety of this process was evaluated with an Advanced Reactive System Screening Tool (ARSST),²¹ and no

self-heating or self-pressurization events were observed up to 160 °C. Since the reaction was run in MeOH, several enol ether intermediates could be detected by HPLC (Scheme 3). At the

Scheme 3. Intermediates Observed in the NCS Chlorination of 6



end of the reaction, 40% of the product exists as the enol ether **11** as determined by ^1H NMR. We believe that the presence of **11** at the end of the reaction provides a rationale for the high selectivity for the desired mono chlorination product. The intermediate **11** can easily be converted back to **2** upon the addition of water during workup, allowing for the isolation of pure **2**.

Step 3. Amidation of Chloroketone 2. Having devised a scale-independent alternative process to access chloroketone **2**, our focus turned to the final amidation step to provide **5** (Scheme 2).²² Due to the high in-process purity of the reactions, the first two steps of the sequence were telescoped, thus avoiding the isolation of compounds **6** and **2**.²³ This allowed for streamlined access to chloroketone **2** via the new route, despite the addition of another step relative to the original Friedel–Crafts acylation with ClCH_2COCl . Conditions for the final amidation²⁴ of α -chloro ketone **2** involved the use of the sodium salt of *N*-formyl tosylamide **4** in the presence of Bu_4NBr in 2-MeTHF.²⁵ The amidation was optimized by carrying out DoE studies focused on the effect of concentration, temperature, water content, equivalents of Bu_4NBr (TBABr) and **4** on the reaction rate, and the final purity profile. Careful analysis of the DoE data revealed that using high substrate concentrations (6 L 2-MeTHF/kg of **2**) and 0.2 equiv of Bu_4NBr at 40 °C allowed for reaction completion in <4 h with an excellent purity profile. Crystallization of **5** demonstrated excellent purging of hydrolysis impurities (typically formed in <1 HPLC AP (area percent) relative to **5**) along with succinimide, allowing for the isolation of **5** in ≥ 98 HPLC AP.

The amidation reaction results in a reactive crystallization which also generates 1 equiv of NaCl as a byproduct. A crystallization was devised that utilized the addition of an antisolvent mixture of isopropanol/water to the Me-THF process stream to maximize the yield and potency of **5** while also purging NaCl. Figure 6 shows a map of the expected isolated yields versus the volumes (L/kg) of IPA and water. The expected isolated yields are based on solubility data and only account for material lost to the mother liquors. The plot shows the isolated yield is a weak function of water content and

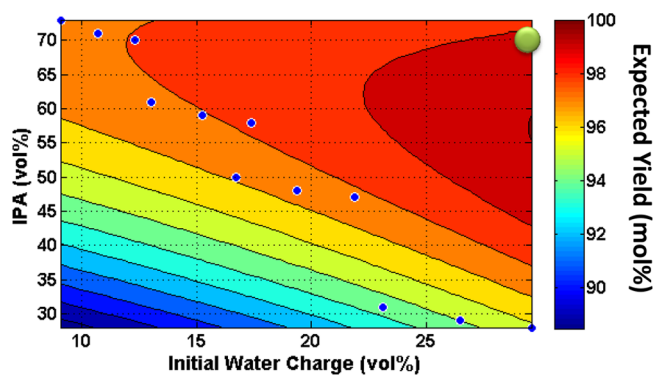
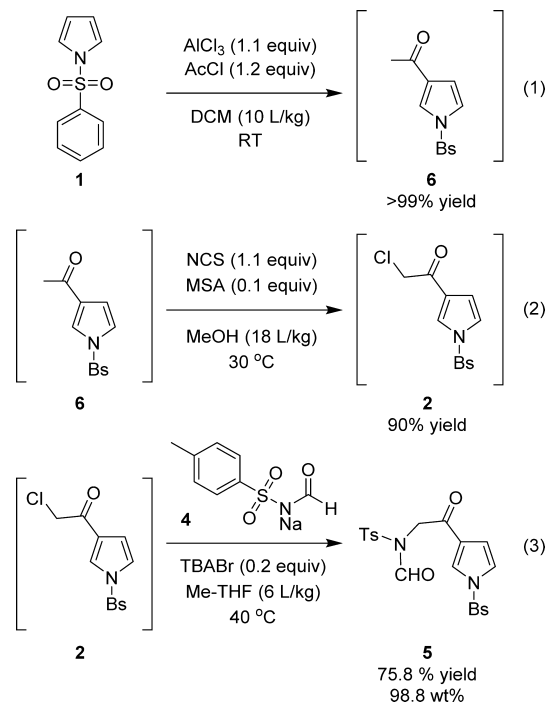


Figure 6. Response of the crystallization of **5** to IPA and water volume %.

a much stronger function of IPA concentration. The isolated yield and potency could be maximized by first charging 30 vol % of water to dissolve the NaCl generated during the reaction and then charging 70 vol % of IPA to maximize the crystallization yield (green circle in Figure 6).

Optimizing the amidation step was the final component to successfully develop a high-yielding, selective, and scale-independent route to **5** (Scheme 4). The commercial viability

Scheme 4. Synthesis of 5



of this three-step process has been demonstrated on a 420 kg scale and has consistently achieved a 62–75% overall yield for the three-step telescope with excellent purity (>98 HPLC AP) and potency (>98 wt %). Compared to the original two-step process, this represents a significant improvement despite the addition of a linear step to the sequence (Table 4).

CONCLUSIONS

Much of process chemistry is focused on streamlining reactions to improve efficiency. For example, improvements in yield, the reduction of solvent usage, and the removal of unit operations

Table 4. Comparison of the Two- and Three-Step Routes to **5**

	original route	commercial route
step 1	ClCH ₂ COCl	AcCl
number of steps	2	3
yield	34%	75%
purity (HPLC)	97–98%	98–99%
process robustness	scale dependent	scale independent

are key deliverables in late phase process development.²⁶ Design of Experiments (DoE) studies are a popular method for performing this kind of optimization. Although this technique has proven powerful and insightful for such fine-tuning of reaction conditions, it may have limitations if the conditions are at a local, rather than a global, optimum. Step changes in terms of reagent choice or route are difficult to predict or support with the statistical outputs of a DoE study. In this report, we describe a scenario where scale-dependent factors led to significant challenges that could not be eliminated through simple variations in the original reaction conditions. While DoE studies led to specific improvements for a given scale and reactor, no general solutions could be found to define a high-yielding process. In an attempt to better understand the root cause of the scale dependence, a series of spectroscopic investigations were undertaken which identified key reaction intermediates and revealed limitations that are inherent to the mechanism of the reaction. These studies also pointed to a path forward, but only if an additional step could be added to the route. Although the proposal to add a step to a synthetic route in planning for a large-scale campaign is not a decision that can be made lightly, a mechanistic explanation of the issues allowed us to build a strong, data-driven case for this change. In the end, the decision to switch from a highly variable and low yielding two-step route to a high-yielding and robust three-step route was made, and the experience at the plant scale has validated that choice.

In summary, we hope that this report emphasizes the importance of deep, fundamental process understanding at scale if robust and reliable processes are the end goal. A first-principles approach allows us to view processes in a more holistic sense and drive decisions which will have significant payoffs in terms of cost and productivity. Exclusive focus on simple metrics like step count may in fact hinder the effort to identify more efficient processes.

■ EXPERIMENTAL SECTION

Preparation of *N*-(2-Oxo-2-(1-(phenylsulfonyl)-1*H*-pyrrol-3-yl)ethyl)-*N*-(phenylsulfonyl)formamide (5**) by the Two-Step Route.** To a reactor under N₂ was charged CH₂Cl₂ (1826 L, 16L/kg based on **1**) followed by addition of aluminum chloride (87.4 kg, 655.46 mol, 1.19 equiv). The suspension was stirred at 15–20 °C for 30 min. Chloroacetyl chloride (62.48 L, 88.6 kg, 784.48 mol, 1.42 equiv) was then added, and the mixture was stirred at 25 °C for 1–2 h until a clear solution was obtained. To this solution was then added a solution of benzenesulfonylpyrrole (**1**) in 228 L CH₂Cl₂ (114.15 kg, 550.81 mol) over 11 min. The resulting solution was heated to 35 °C and aged for 5 h or until full conversion was obtained as confirmed by HPLC. The solution was cooled to 10–20 °C and then slowly transferred to another reactor containing water (1369 L, 12 L/kg based on **1**) at 5–10 °C, at such a rate as to maintain an internal temperature below 20 °C.

The resulting biphasic mixture was stirred at 20–25 °C for 0.5–1 h. The organic layer was separated and washed sequentially with 5 wt % sodium carbonate solution (1141 L, 10 L/kg) and water (1141 L, 10 L/kg). The organic layer was concentrated under vacuum to 3–4 L/kg while maintaining the batch temperature below 40 °C. To this solution was added THF (1141 L, 10 L/kg), and then it was concentrated to 3–4 L/kg under vacuum. After the batch was cooled to 25–30 °C, THF (685 L, 6 L/kg) was added. The water content of the crude solution was 2 wt % H₂O as determined by Karl Fischer titration. The solution yield of **2** was 71.3%, and in-process purity was 90.3 AP. To this solution of **2** was added the sodium salt of *N*-formyl-*p*-toluene sulfonamide **4** (110.5 kg, 499.97 mol, 0.9 equiv), followed by tetra-*n*-butyl ammonium bromide (13.4 kg, 41.56 mol, 0.07 equiv). The resulting suspension was heated to 60 °C and aged for 4 h or until full conversion was obtained as confirmed by HPLC. The suspension was then cooled to 25 °C and washed with 0.5 wt % HCl solution containing 5% brine (685 L, 6 L/kg) and then brine (685 L, 6 L/kg). The organic layer was concentrated under vacuum to 7 L/kg. To perform the crystallization, isopropanol (650.6 L, 5.7 L/kg) was charged at 25 °C. The batch was then seeded with 0.05 wt % **5** and stirred for 30 min to generate a suspension. A second charge of isopropanol (650.6 L, 5.7 L/kg) was then added, and the mixture was stirred at 25 °C for 2 h. A thick slurry was obtained, which was cooled to 10–15 °C and stirred for 2 h prior to filtration. The cake was washed with chilled 1.75:1 IPA/THF (10–15 °C, 342.5 L, 3 L/kg) followed by 2:1 IPA/THF (10–15 °C, 456.6 L, 4 L/kg). The wet cake was dried at 50 °C under N₂/vacuum sweep to reach LOD < 0.5%, and **5** was isolated as a white crystalline solid (85 kg, 34.3% yield, 98.0 AP). Mp 145 °C. ¹H NMR (DMSO-*d*₆) 9.18 (br, 1H), 8.43 (m, 1H), 8.09 (m, 2H), 7.90 (m, 2H), 7.81 (m, 1H), 7.70 (m, 2H), 7.50–7.42 (m, 3H), 6.67 (m, 1H), 4.91 (br, 2H), 2.41 (s, 3H). ¹³C NMR (DMSO-*d*₆) 184.6, 160.8, 145.8, 137.9, 134.9, 134.8, 130.3, 129.9, 127.9, 127.4, 125.6, 124.4, 121.9, 112.2, 48.3, 21.8. HRMS elemental calculated for C₂₀H₁₈N₂O₆S₂: 447.0679; found: 447.0677.

Preparation of *N*-(2-Oxo-2-(1-(phenylsulfonyl)-1*H*-pyrrol-3-yl)ethyl)-*N*-(phenylsulfonyl)formamide (5**) by the Three-Step Route.** To a reactor under N₂ was charged CH₂Cl₂ (3384 L, 8 L/kg), followed by addition of aluminum chloride (229.3 kg, 1719.6 mol, 1.1 equiv). The resulting suspension was held at 20 °C. Acetyl chloride (133.3 L, 147.2 kg, 1875.15 mol, 1.2 equiv) was added to the suspension, and it was stirred at 20 °C until a clear solution was obtained (~1 h). To this solution was then added a solution of benzenesulfonylpyrrole (**1**) in 850 L of CH₂Cl₂ (423 kg, 1563.27 mol) over 60 min to control off-gassing (1 equiv HCl). The homogeneous reaction was stirred at 20 °C for 1 h or until >99% conversion was obtained as confirmed by HPLC. The solution was cooled to 10–20 °C and then slowly transferred to another reactor containing water (2115 L, 5 L/kg based on **1**) at 5–10 °C, at such a rate as to maintain an internal temperature below 20 °C. The biphasic mixture was stirred vigorously at 20 °C for at least 1 h. The organic phase was separated, and a vacuum distillation was performed to obtain a water content of <0.05 wt % H₂O as determined by Karl Fischer titration. Methanol (2538L, 6 L/kg) was then added, and CH₂Cl₂ was removed by vacuum distillation until less than <0.05 wt % CH₂Cl₂ could be detected by GC analysis. Methanol was added to adjust the final volume to 18 L/kg (~7600 L), and the water content of the solution was controlled at <0.15 wt % H₂O as determined by Karl

Fischer titration. The solution was cooled to 20 °C. The solution yield of **6** was >99%, and the in-process purity was 99 AP. To this MeOH solution of **6** was added *N*-chlorosuccinimide (219.2 kg, 1641.57 mol, 1.05 equiv) followed by methanesulfonic acid (13.64 L, 18 kg, 187.28 mol, 0.12 equiv). The mixture was heated to 30 °C and aged for 6 h or until >97% conversion was obtained as confirmed by HPLC. The solution was cooled to 20 °C, and water (65 L, 0.2 L/kg) was added. The solution was concentrated under vacuum to 5 L/kg for addition of 2-MeTHF (3250 L, 10 L/kg). The resulting solution was stirred at 20 °C for 1 h to effect cleavage of the enol ether **11**. Methanol was removed by vacuum distillation to achieve a 10 L/kg 2-MeTHF solution of **2** containing less than 1 wt % MeOH while maintaining the internal temperature below 40 °C. The solution was washed with 20 wt % NaCl solution (1625 L, 5 L/kg) containing 0.15 equiv of sodium bicarbonate (19.7 kg, 234.49 mol). The organic layer was distilled under vacuum to obtain a water content of <0.03 wt % H₂O as determined by Karl Fischer titration. The batch was cooled to 20 °C, and 2-MeTHF was added to a final volume to 6 L/kg (~1900 L). The solution yield of **2** was 90%, and the in-process purity was 93 AP. To this 2-MeTHF solution of **2** was added the sodium salt of *N*-formyl-*p*-toluene sulfonamide **4** (345.8 kg, 1564.6 mol, 1.0 equiv) and TBABr (100.8 kg, 312.68 mol, 0.2 equiv). The resulting suspension was heated to 40–50 °C and aged 1 h or until >99% conversion was obtained as confirmed by HPLC. To the solution was added 2:1 IPA/water (8400 L, 20 L/kg) over 1 h while maintaining its temperature at 40 °C. The mixture was aged at 40 °C for 1 h then cooled to 20 °C over 1 h and held at 20 °C for no less than 2 h. The resulting slurry was filtered and washed with IPA (2100 L, 2 × 5 L/kg). The wet cake was dried at 50 °C under N₂/vacuum sweep to reach LOD < 0.5%, and **5** was isolated as a white crystalline solid⁵ (529.1 kg, 75.8% yield, 98.8 AP).

■ ASSOCIATED CONTENT

Supporting Information

The Supporting Information is available free of charge on the ACS Publications website at DOI: [10.1021/acs.oprd.7b00115](https://doi.org/10.1021/acs.oprd.7b00115).

Experimental procedures, characterization data, and ¹H and ¹³C NMR data (PDF)

■ AUTHOR INFORMATION

Corresponding Author

*E-mail: gregory.beutner@bms.com.

ORCID

Gregory L. Beutner: 0000-0001-8779-1404

Michael Bultman: 0000-0002-0140-6120

Martin D. Eastgate: 0000-0002-6487-3121

Notes

The authors declare no competing financial interest.

■ ACKNOWLEDGMENTS

The authors thank Dr. Frank A. Rinaldi for his assistance with NMR spectroscopy, Dr. Wei Ding and Mr. Mike Peddicord for assistance with mass spectroscopy, Drs. Brendan Mack and Jose Tabora for assistance with DoE planning, Dr. Jacob Janey for assistance with lab automation, and Dr. Sergei Kolotuchin for helpful discussions. We thank Dr. Michael Schmidt for a careful review of this manuscript and for providing helpful suggestions

on the content. We thank the Chemical & Synthetic Development senior management for support during the preparation of this manuscript.

■ REFERENCES

- (1) (a) Li, J. J. *Heterocyclic Chemistry in Drug Discovery*; Wiley: Hoboken, NJ, 2013; pp 18–53. (b) Young, I. S.; Thornton, P. D.; Thompson, A. *Nat. Prod. Rep.* **2010**, *27*, 1801–1839. (c) Lipkus, A. H.; Yuan, Q.; Lucas, K. A.; Funk, S. A.; Bartelt, W. F., III; Schenck, R. J.; Trippe, A. J. *J. Org. Chem.* **2008**, *73*, 4443–4451.
- (2) (a) Estevez, V.; Villacampa, M.; Menendez, J. C. *Chem. Soc. Rev.* **2010**, *39*, 4402–4421. (b) Bergman, J.; Janosik, T. In *Comprehensive Heterocyclic Chemistry III*; Jones, G., Ramsden, C. A., Eds.; Elsevier: Amsterdam, 2008; Vol. 3, pp 269–351.
- (3) (a) Anderson, H. J.; Loader, C. E. *Synthesis* **1985**, *1985*, 353–364. (b) Jones, R. A.; Bean, G. P. *The Chemistry of Pyrroles*; Academic Press: London, 1977; pp 115–208.
- (4) (a) Gutierrez, E. G.; Wong, C. J.; Sahin, A. H.; Franz, A. K. *Org. Lett.* **2011**, *13*, 5754–5757. (b) de Haro, T.; Nevado, C. *J. Am. Chem. Soc.* **2010**, *132*, 1512–1513. (c) Tobisu, M.; Yamaguchi, S.; Chatani, N. *Org. Lett.* **2007**, *9*, 3351–3353. (d) Pirrung, M. C.; Zhang, J.; Lackey, K.; Sternbach, D. D.; Brown, F. J. *Org. Chem.* **1995**, *60*, 2112–2124. (e) Bray, B. L.; Mathies, P. H.; Naef, R.; Solas, D. R.; Tidwell, T. T.; Artis, D. R.; Muchowski, J. M. *J. Org. Chem.* **1990**, *55*, 6317–6328.
- (5) (a) Chen, K.; Risatti, C.; Bultman, M. S.; Soumeillant, M.; Simpson, J.; Zheng, B.; Fanfair, D.; Mahoney, M.; Mudryk, B.; Fox, R. J.; Hsiao, Y.; Murugesan, S.; Conlon, D. A.; Buono, F. G.; Eastgate, M. D. *J. Org. Chem.* **2014**, *79*, 8757–8767. (b) Eastgate, M. D.; Bultman, M. S.; Chen, K. C.; Fanfair, D. D.; Fox, R. J.; La Cruz, T. E.; Mudryk, B. M.; Risatti, C. A.; Simpson, J. H.; Soumeillant, M. C.; Tripp, J. C.; Xiao, Y. Methods for the Preparation of HIV Attachment Inhibitor Piperazine Prodrug Compound. U.S. Patent 2013/0203992. (c) See [10.1021/op7b00121](https://doi.org/10.1021/op7b00121).
- (6) (a) Silvestri, R.; Pifferi, A.; De Martino, G.; Massa, S.; Saturnino, C.; Artico, M. *Heterocycles* **2000**, *53*, 2163–2174. (b) De Micheli, C.; De Amici, M.; Locati, S. *Il Farmaco* **1984**, *39*, 277–288.
- (7) Atherton, J. H.; Carpenter, K. J. In *Process Development: Physicochemical Concepts*; Oxford University Press: Oxford, England, 2005; pp 36–53.
- (8) Due to time constraints, the initial campaign was completed using the ClCH₂COCl procedure, and a total of thirteen 120 kg scale batches were processed that consistently gave a ~70% yield of **2**.
- (9) ReactIR experiments were performed in DCE to minimize evaporation of DCM during long experiment times.
- (10) Germain, A.; Commeyras, A.; Casadevall, A. *J. Chem. Soc. D* **1971**, *0*, 633–635.
- (11) The solubility of HCl in DCE at 20 °C is reported as 0.53 mmol/mL; see: Ahmed, W.; Gerrard, W.; Maladkar, V. K. *J. Appl. Chem.* **1970**, *20*, 109–116.
- (12) Jones, B.; Nachtsheim, C. J. *J. Qual. Technol.* **2011**, *43*, 1–15.
- (13) For the DOE study, MeOH was premixed with AlCl₃ in DCM prior to the reaction to simulate the addition of HCl.
- (14) Huffman, J. W.; Smith, V. J.; Padgett, L. W. *Tetrahedron* **2008**, *64*, 2104–2112.
- (15) Kakushima, M.; Hamel, P.; Frenette, R.; Rokach, J. *J. Org. Chem.* **1983**, *48*, 3214–3219.
- (16) For examples with acylating reagents, see: (a) Noland, W. E.; Lanzatella, N. P. *J. Heterocycl. Chem.* **2009**, *46*, 1285–1295. (b) Harrak, Y.; Rosell, G.; Daidone, G.; Plescia, S.; Schillaci, D.; Pujol, M. D. *Bioorg. Med. Chem.* **2007**, *15*, 4876–4890. (c) Muratake, H.; Natsume, M. *Heterocycles* **1990**, *31*, 683–690. (d) De Micheli, C.; De Amici, M.; Platini, D. B. *Il Farmaco* **1986**, *41*, 913–925. (e) Anderson, H. J.; Loader, C. E.; Xu, X. R.; Le, N.; Gogan, N. J.; McDonald, R.; Edwards, L. G. *Can. J. Chem.* **1985**, *63*, 896–902. (f) Xu, X. R.; Anderson, H. J.; Gogan, N. J.; Loader, C. E.; McDonald, R. *Tetrahedron Lett.* **1981**, *22*, 4899–4900.
- (17) Bigi, F.; Casnati, G.; Sartori, G.; Predieri, G. *J. Chem. Soc., Perkin Trans. 2* **1991**, *2*, 1319–1321.

(18) (a) Shi, X.-X.; Dai, L.-X. *J. Org. Chem.* **1993**, *58*, 4596–4598. (b) Kajigaeshi, S.; Kakinami, T.; Moriwaki, M.; Fujisaki, S.; Maeno, K.; Okamoto, T. *Synthesis* **1988**, 1988, 545–546. (c) Chen, Z.; Zhou, B.; Cai, H.; Zhu, W.; Zou, X. *Green Chem.* **2009**, *11*, 275–278. (d) Xu, Z.; Zhang, D.; Zou, X. *Synth. Commun.* **2006**, *36*, 255–258.

(19) Zhou, Z. S.; Li, L.; He, X. H. *Chin. Chem. Lett.* **2012**, *23*, 1213–1216.

(20) (a) Lee, J. C.; Park, H. J. *Synth. Commun.* **2007**, *37*, 87–90. (b) Wang, C.; Tunge, J. *Chem. Commun.* **2004**, *23*, 2694–2695. (c) Meshram, M.; Reddy, P. N.; Sadashiv, K.; Yadav, J. S. *Tetrahedron Lett.* **2005**, *46*, 623–626. (d) Sreedhar, B.; Surendra Reddy, P.; Madhavi, M. *Synth. Commun.* **2007**, *37*, 4149–4156.

(21) Advanced Reactive System Screening Tool (ARSST). Burelbach, J. P. *North American Thermal Analysis Society, 28th Conference*, Orlando, FL, Oct. 4–6, 2000.

(22) Hoffmann, R. W.; Bruckner, D. *New J. Chem.* **2001**, *25*, 369–373.

(23) Compound **2** has been shown to be a potent skin sensitizer (local lymph node assay EC₃ = 0.028%).

(24) (a) Li, X.; Zhou, X.; Zhang, J.; Wang, L.; Long, L.; Zheng, Z.; Li, S.; Zhong, W. *Molecules* **2014**, *19*, 2004–2028. (b) van Zupten, S.; Kraus, M.; Driessen, C.; van der Marel, G. A.; Overkleeft, H. S.; Reedijk, J. J. *Inorg. Biochem.* **2005**, *99*, 1384–1389. (c) Adam, I.; Orain, D.; Meier, P. *Synlett* **2004**, *11*, 2031–2033. (d) Mitschke, U.; Debaerdemaeker, T.; Baeuerle, P. *Eur. J. Org. Chem.* **2000**, *2000*, 425–437.

(25) For examples of the use of catalytic TBABr in chloroketone amidations, see: Aldous, S.; Fennie, M. W.; Jiang, J. Z.; John, S.; Mu, L.; Pedgrift, B.; Pribish, J.; Rauckman, B.; Sabol, J. S.; Stoklosa, G. T.; Thurairatnam, S.; van Deusen, C. L. *Pyrimidine Hydrazine Compounds as PGDS Inhibitors*. WIPO, WO 2008/121670 A1..

(26) Weissman, S. A.; Anderson, N. G. *Org. Process Res. Dev.* **2015**, *19*, 1605–1633.